Chinese Chemical Letters 35 (2024) 109127

Contents lists available at ScienceDirect

Chinese Chemical Letters

journal homepage: www.elsevier.com/locate/cclet

Differentiated self-assembly through orthogonal noncovalent interactions towards the synthesis of two-dimensional woven supramolecular polymers

Zhenzhu Wang[a,b], Chenglong Liu[a,b], Yunpeng Ge[a,b], Wencan Li[a,b], Chenyang Zhang[a,b], Bing Yang[a], Shizhong Mao[a], Zeyuan Dong[a,b,*]

[a] State Key Laboratory of Supramolecular Structure and Materials, College of Chemistry, Jilin University, Changchun 130012, China
[b] Center for Supramolecular Chemical Biology, Jilin University, Changchun 130012, China

ARTICLE INFO

Article history:
Received 5 June 2023
Revised 12 September 2023
Accepted 20 September 2023
Available online 21 September 2023

Keywords:
Differentiated self-assembly
Double-stranded helix
Molecular weaving
Supramolecular chemistry
Two-dimensional polymer

ABSTRACT

Molecular weaving is a powerful approach to make molecularly woven materials that have showed unprecedented characteristics and properties intrinsically distinct to those of non-woven materials. We here report a facile and efficient approach for the synthesis of 2D woven supramolecular polymers by differentiated self-assembly through orthogonal noncovalent interactions. Importantly, the difference in binding strength of two orthogonal noncovalent interactions can be used to control the process of molecular weaving. Consequently, single-layered 2D woven supramolecular polymers were synthesized and fully characterized by various techniques. This study demonstrates a controllable method for molecular weaving, and will significantly hasten the development of molecularly woven materials.

© 2024 Published by Elsevier B.V. on behalf of Chinese Chemical Society and Institute of Materia Medica, Chinese Academy of Medical Sciences.

Fiber weaving is a conventional practical technique for fabric production that has been widely applicable in the various fields such as textiles, electronic devices, architectures, medicine, ocean, and aerospace in real life. Like fiber weaving, molecular weaving is a molecule-level technological process that is emerging as a potentially powerful approach to achieve the landscape of molecular fabrics. Chemists worldwide are devoted in the aim of constructing unique molecular fabrics in two or three dimensions [1–16], because molecular fabrics possess intrinsically distinctive topological structures and features differing from molecular strands interlaced. Recently, molecular weaving in two dimensions or three dimensions has been investigated [17–21]. For example, Yaghi and coworkers developed a class of diaxially woven covalent organic frameworks (COFs) by means of metal template synthesis [22–24]. Besides the strategy of diaxial molecular weaves, Lewandowska *et al.* reported a triaxial supramolecular weave approach, which leads to the formation of a wholly organic micrometer-scale weave with layer height exceeding 100 nm [21]. In addition, a dynamic 2D woven hydrogen-bonded organic framework through the interlocking of 1D strands by O–H···O hydrogen bonds had been recently reported [20]. Notably, the weak single H-bond is responsible to exceptional dynamics of the molecularly woven crystal, but this is not sufficiently robust for molecular weaving in solution. Recently, Leigh and coworkers reported a self-assembled layered woven material consisting of alternating aliphatic and aromatic segmented polymer strands that interweave each other within discretelayers [19]. In the work, the strategy of regional weave realizes a woven material with defined arrangement of 1D strands in the manner of a macroscopic textile. With the access of these molecularly woven materials, it is eager to develop versatile and facile approaches for the synthesis of large-sized 2D woven polymers.

Advances in molecularly woven materials have showed unprecedented characteristics and properties that are intrinsically distinct to those of non-woven materials [11]. The synthesis of 2D woven polymers therefore stands in the way of molecularly woven material development. Among few reported examples [11,25–32], the design of noncovalently intercrossing pattern is vital to construct molecularly woven structures. As reported in the literatures [12,18,33,34], using ion-based template for the pre-synthesis of noncovalently intercrossing patterns becomes a main mode of molecular weaving. Therefore, it is important to discover appropriate molecular entities that can form an intercrossing pattern at the molecular level. As known, the formation of double-stranded helix by the metal-free dimerization of single-stranded helix presents a feasible mode to generate an intercrossing pattern. Moreover, the presence of helical skeleton in woven structures weakens nonco-

* Corresponding author at: State Key Laboratory of Supramolecular Structure and Materials, College of Chemistry, Jilin University, Changchun 130012, China.
E-mail address: zdong@jlu.edu.cn (Z. Dong).

https://doi.org/10.1016/j.cclet.2023.109127
1001-8417/© 2024 Published by Elsevier B.V. on behalf of Chinese Chemical Society and Institute of Materia Medica, Chinese Academy of Medical Sciences.

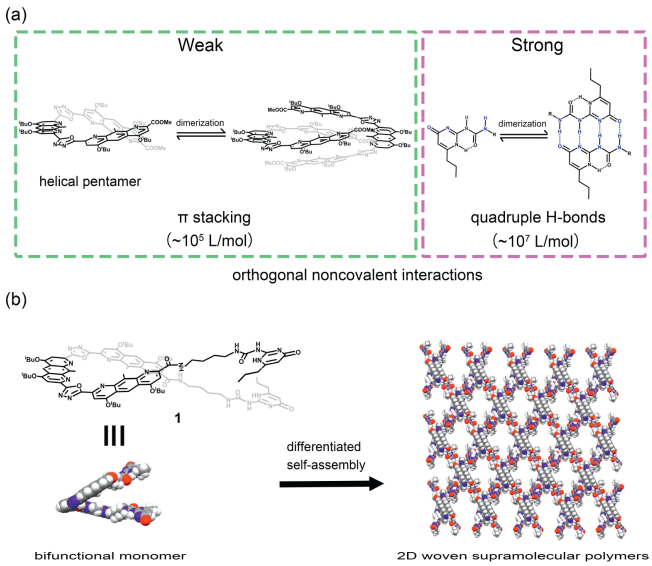

Fig. 1. (a) Molecular structure of helical pentamer and two kinds of noncovalent interactions with different binding constants are used to synthesize 2D woven supramolecular polymers *via* differentiated self-assembly of orthogonal noncovalent interactions. The relevant values of the binding constants of different noncovalent interactions are derived from literature reports [55,56]. (b) Chemical structure and molecular simulation of bifunctional monomer **1** as well as the schematic diagram of the formation of 2D woven supramolecular polymers by orthogonal π-π interactions and hydrogen bonding. Color code: gray, C; blue, N; red, O; white, H.

valent interactions between layers, thus possibly obtaining free-standing single-layered woven structures. It is known that hydrogen bonding and π-π interactions were commonly used in supramolecular assembly because these two noncovalent driving forces are essentially orthogonal and could be differentiated in binding strength [35–53]. Herein, we report a facile and efficient approach for the synthesis of 2D woven supramolecular polymers by differentiated self-assembly through orthogonal noncovalent interactions. In particular, we employ an aromatic helix pentamer that can spontaneously dimerize into double-stranded helix *via* π-π interactions with a dimerization constant of 10^5 L/mol in chloroform, to act as a noncovalently intercrossing pattern (Fig. 1a) [54,55]. At the same time, the quadruple hydrogen bonding ureidopyrimidinone (UPy) unit developed by the Meijer group is used for noncovalently crosslinking group because of its high association constant of 10^7 L/mol in chloroform (Fig. 1a) [56]. The difference in binding strength of these two orthogonal noncovalent interactions will provide possibility to control the process of molecular weaving, even though the synergic combination of hydrogen bonding and π-π interactions was not explored in molecular weaving. In fact, it is the first design concept to controllable molecular weaving. Therefore, by integrating aromatic helix pentamer and UPy units into a bifunctional monomer that could form in prior 1D supramolecular polymer strands by strong quadruplex H-bonds and then mutually interlace through the formation of double-stranded helix by relatively weak π-π interactions, 2D woven supramolecular polymers will be spontaneously prepared by differentiated noncovalent synthesis (Fig. 1).

With the design in mind, a bifunctional monomer **1** consisting of aromatic helical segment and two UPy units was prepared through multistep organic synthesis and fully characterized (see Supporting information for details). The aromatic helical segment of bifunctional monomer **1** spontaneously dimerizes into double-stranded helix that forms a noncovalently intercrossing pattern available for molecular weaving [54,55], which can be supported by molecular simulation (Fig. S1 in Supporting information). To further monitor this process, concentration-dependent fluorescence titrations of pentamer and monomer **1** were performed. The fluorescence intensity of emission wavelength at 473 nm gradually increases and afterward turns to decrease while increasing the concentration of pentamer (Figs. 2a and b). This indicates the formation of double-stranded helix *via* π-π interactions with transition concentration of 30 μmol/L (Fig. 2c). Similar results can be observed in fluorescence spectra of monomer **1** (Figs. 2d and e), but the transition concentration obviously increases to 45 μmol/L (Fig. 2f), which is about 50% higher than that of pentamer. Notably, for monomer **1** at the transition concentration of 45 μmol/L, UPy-based 1D supramolecular polymers have formed owing to its association constant of 10^7 L/mol. This suggests that the prior formation of H-bonded supramolecular polymer strands slightly weakens π-π interactions of aromatic helices. Nevertheless, the tran-

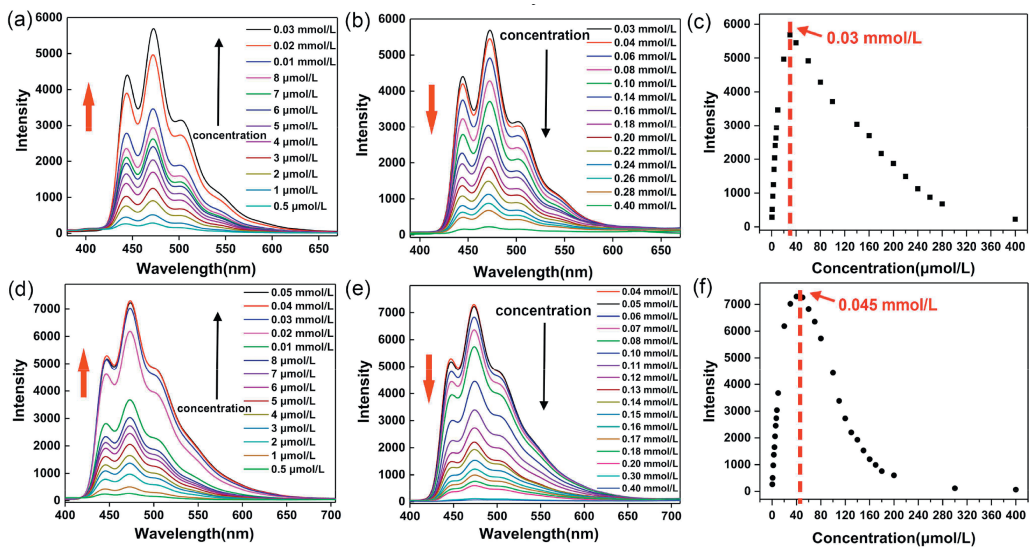

Fig. 2. Fluorescence spectra of helical pentamer at different concentrations (a) from 0.5 μmol/L to 0.03 mmol/L and (b) from 0.03 mmol/L to 0.4 mmol/L at 298 K in chloroform at an excitation wavelength of 360 nm. (c) Plot curve of the fluorescence intensity at different concentrations of helical pentamer at 473 nm. Fluorescence spectra of monomer **1** at different concentrations (d) from 0.5 μmol/L to 0.05 mmol/L and (e) from 0.04 mmol/L to 0.4 mmol/L at 298 K in chloroform at an excitation wavelength of 360 nm. (d) Plot curve of the fluorescence intensity at different concentrations of monomer **1** at 473 nm.

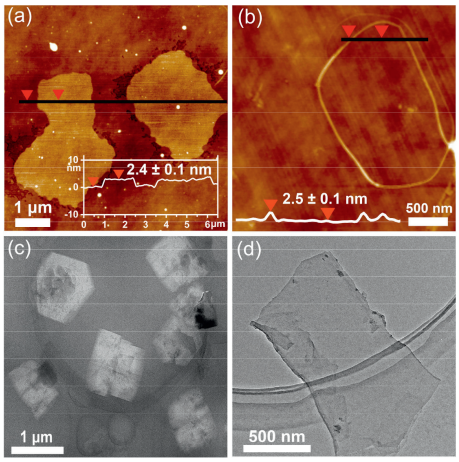

Fig. 3. (a) AFM image of the self-assembled nanosheets of monomer **1**. The samples were prepared by using anhydrous chloroform solution of **1**. (b) AFM image of self-assembled nanowires of helical pentamer in anhydrous chloroform. The white line in the image represents the height profile of 1D nanowires. (c) Cryo-TEM images of free-standing nanosheet structures formed *via* noncovalently intercrossing mode of monomer **1** in anhydrous DMF. (d) TEM image of 2D nanosheets by self-assembly of monomer **1** in anhydrous DMF.

sition concentration corresponds to the π-stacking dimerization constant of about 10^5 L/mol, which is consistent with previous results [55]. In addition, concentration-dependent UV–vis spectra of monomer **1** demonstrated that the transition concentration of single-stranded helix to double-stranded helix is 45 μmol/L (Fig. S2 in Supporting information), according with the result of fluorescence titrations.

Dynamic light scattering (DLS) experiments supported the self-assembly ability of monomer **1** in solution. When the concentration of monomer **1** changes from 0.4 μmol/L to 0.3 mmol/L, the size of assemblies gradually increases to 900 nm (Fig. S3 in Supporting information). The assembling structure of monomer **1** was observed by atomic force microscopy (AFM). As seen in Fig. 3a, the self-assembly of monomer **1** gives rise to the formation of 2D supramolecular polymers with uniform thickness of 2.4 nm in chloroform. Surprisingly, the outer diameter (~2.5 nm) of helical segments coincides with the thickness of 2D supramolecular polymers, indicating a single-layered structure. In contrast, the self-assembly of helical pentamer just generates 1D nanowires (Fig. 3b). In essential, the formation of single-layered 2D supramolecular polymers can be reasonably achieved by molecular weaving. Additionally, the micrometer-scale 2D supramolecular polymers show remarkable aspect ratio of exceeding 1000:1 (Fig. 3a). In order to directly observe the assembling structure of monomer **1** in solution, cryo-TEM experiment was carried out. As seen in Fig. 3c, micrometer-scale sheet-like structures by self-assembly of monomer **1** were clearly observed in anhydrous DMF. Notably, the self-assembled 2D nanostructures (Fig. 3c) of monomer **1** in DMF have more regular edges than that (Fig. 3a) in chloroform. The difference in the self-assembled morphologies of monomer **1** is caused by solvation effect. As evidenced by optical micrograph (Fig. S4 in Supporting information), the self-assembled morphology of monomer **1** presents regular edge in DMF, whereas apparently disordered morphology was observed in chloroform. Furthermore, the self-assembled structures of monomer **1** were studied by transmission electron microscopy (TEM). As shown in Fig. 3d, micrometer-scale 2D nanostructures were obtained by self-assembly of monomer **1**. These above observations clearly demonstrate the formation of single-layered 2D supramolecular polymers designed by molecular weaving.

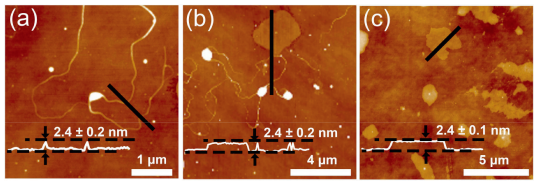

Fig. 4. Monitoring the formation of nanosheets by AFM. Effect of bifunctional monomer **1** concentration on the formation of nanosheets: AFM images of the nanosheets prepared by polymerization of **1** in anhydrous $CHCl_3$ at different concentrations: 0.1 μmol/L (a), 10 μmol/L (b) and 50 μmol/L (c). Schematic representation of the proposed growth mechanism of the nanosheet: helical segment and flexible UPy units form 1D supramolecular polymer strands driven by strong hydrogen bonding forces and further grows to the self-assembled 2D nanostructures under weak π-π interactions.

Next, the process of controllable molecular weaving was investigated since the orthogonal noncovalent interactions possess nearly two orders of magnitude difference in binding strength. As shown in AFM (Fig. 4a), 1D supramolecular polymer strands generate in prior by strong H-bonds when the concentration of monomer **1** is below 0.1 μmol/L. By increasing the concentration of monomer **1**, both 1D and single-layered 2D supramolecular polymers can be simultaneously observed, and woven intermediates can also be detected (Fig. 4b). When the concentration of monomer **1** exceeds 50 μmol/L, 1D polymer strands are almost undetectable, and single-layered 2D supramolecular polymers completely dominate in the self-assembled structures of monomer **1** (Fig. 4c). Apparently, subsequent molecular weaving process of UPy-based supramolecular polymer strands does take place *via* the formation of double-stranded helix by π-π interactions. In addition, ^{1}H NMR spectrum of monomer **1** at the concentration of 6 mmol/L at 298 K, shows a set of unique and dispersed proton signals that corresponds to discrete, molecularly woven structures (Fig. S16 in Supporting information). This suggests that the aromatic helix units are stochastically fixed into molecularly woven 2D architecture. In contrast, aromatic helix without UPy units gives a set of wide proton NMR signals, indicative of π-stacking aggregate structures (Fig. S5 in Supporting information). Moreover, by adding a small amount of trifluoroacetic acid (TFA) into the solution of monomer **1**, the structure of noncovalently woven 2D supramolecular polymers completely breaks down, and free monomer **1** regenerates as observed in ^{1}H NMR spectrum (Fig. S17 in Supporting information). The above results indicate that the process of molecular weaving can be controlled by differentiated self-assembly, and orthogonal noncovalent synthesis provides a facile and efficient strategy for constructing 2D woven supramolecular polymers.

Attempt to directly observe atomic structure (Fig. 5a) of single-layered woven supramolecular polymers failed by TEM, due to the low contrast of pure organic material and the destruction of electron beam as well. Fortunately, the fine structure of four stacked layers from single-layered 2D supramolecular polymers was revealed by TEM (Figs. 5b and c). The four stacked layers present a highly ordered, intercrossed structure with periodic spacing distances of 0.46 and 0.27 nm, respectively. Moreover, as seen in Fig. 5d, the selected area electron diffraction (SAED) pattern clearly exhibits periodic spacing distances of 0.4 and 0.27 nm, according with the four-layered stacking structure of single-layered 2D supramolecular polymers. These results demonstrate that self-assembly of monomer **1** leads to the formation of single-layered 2D woven supramolecular polymers.

In summary, we report a facile and efficient approach for the synthesis of 2D woven supramolecular polymers by differentiated self-assembly through orthogonal noncovalent interactions. To design 2D woven supramolecular polymers, double-stranded helix formed by relatively weak π-π interactions (10^5 L/mol) was used

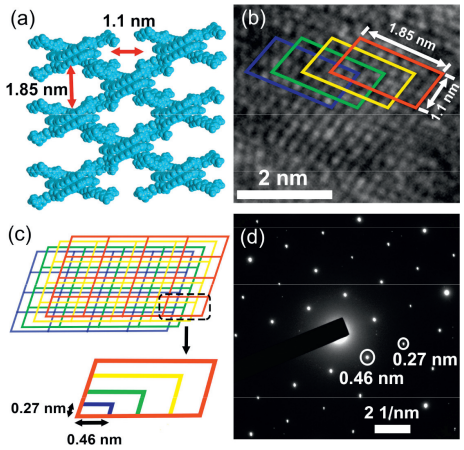

Fig. 5. (a) Molecular simulation of the morphology of self-assembled monomer **1** at equilibrium steady state, shows the periodic spacing distances of monolayered woven structures. (b) The HRTEM image of monomer **1**. (c) The schematic illustration of periodic spacing distances of four stacked layers. (d) The selected area electron diffraction (SAED) pattern of monomer **1**. The samples were prepared by using anhydrous DMF solution of **1** at the concentration of 10^{-4} mol/L.

as a noncovalently intercrossing pattern, and the UPy unit with strong quadruple H-bonding interactions (10^7 L/mol) was employed for noncovalently crosslinking group. Our study demonstrates that the difference in binding strength of two orthogonal noncovalent interactions can be used to control the process of molecular weaving. To our knowledge, this is the first instance of controllable molecular weaving *via* differentiated self-assembly. At the same time, the presence of helical skeleton in woven structures weakens noncovalent interactions between layers, thus achieving the synthesis of single-layered 2D woven supramolecular polymers. This proof-of-concept study introduces a feasible approach to prepare 2D molecularly woven structures, and will significantly hasten the development of molecularly woven materials.

Declaration of competing interest

The authors declare that they have no known competing financial interests or personal relationships that could have appeared to influence the work reported in this paper.

Acknowledgment

This work was supported by the National Natural Science Foundation of China (Nos. 92156012 and 22071078).

Supplementary materials

Supplementary material associated with this article can be found, in the online version, at doi:10.1016/j.cclet.2023.109127.

References

[1] S.R. Batten, R. Robson, Angew. Chem. Int. Ed. 37 (1998) 1460–1494.
[2] L. Carlucci, G. Ciani, D.M. Proserpio, Coord. Chem. Rev. 246 (2003) 247–289.
[3] E.A. Axtell, J.H. Liao, M.G. Kanatzidis, Inorg. Chem. 37 (1998) 5583–5587.
[4] L. Carlucci, G. Ciani, A. Gramaccioli, et al., CrystEngComm 29 (2000) 1–10.
[5] Y. Li, C. Su, A.M. Goforth, et al., Chem. Commun. 9 (2003) 1630–1631.
[6] L. Han, Y. Zhou, Inorg. Chem. Commun. 11 (2008) 385–387.
[7] H. Wu, J. Yang, Z.M. Su, et al., J. Am. Chem. Soc. 133 (2011) 11406–11409.
[8] A.M. Champsaur, C. Mézière, M. Allain, et al., J. Am. Chem. Soc. 139 (2017) 11718–11721.
[9] T. Ciengshin, R. Sha, N.C. Seeman, Angew. Chem. Int. Ed. 50 (2011) 4419–4422.
[10] P. Calcar, M.M. Olmstead, A.L. Balch, J. Chem. Soc., Chem. Commun. 17 (1995) 1773–1774.
[11] Z.H. Zhang, B.J. Andreassen, D.P. August, et al., Nat. Mater. 21 (2022) 275–283.
[12] J.F. Ayme, J.E. Beves, C.J. Campbell, et al., Chem. Soc. Rev. 42 (2013) 1700–1712.
[13] Y. Liu, M. O'Keeffe, M.M.J. Treacy, et al., Chem. Soc. Rev. 47 (2018) 4642–4664.
[14] L. Carlucci, G. Ciani, D.M. Proserpio, et al., Chem. Rev. 114 (2014) 7557–7580.
[15] T.K. Maji, R. Matsuda, S. Kitagawa, Nat. Mater. 6 (2007) 142–148.
[16] B. Chen, M. Eddaoudi, S.T. Hyde, et al., Science 291 (2001) 1021–1023.
[17] Y. Liu, C.S. Diercks, Y. Ma, et al., J. Am. Chem. Soc. 141 (2019) 677–683.
[18] G. Li, L. Wang, L. Wu, et al., J. Am. Chem. Soc. 142 (2020) 14343–14349.
[19] D.P. August, R.A.W. Dryfe, S.J. Haigh, et al., Nature 588 (2020) 429–435.
[20] Q. Huang, W. Li, Z. Mao, et al., Chem 7 (2021) 1321–1332.
[21] U. Lewandowska, W. Zajaczkowski, S. Corra, et al., Nat. Chem. 9 (2017) 1068–1072.
[22] Y. Liu, Y. Ma, Y. Zhao, et al., Science 351 (2016) 365–369.
[23] Y. Zhao, L. Guo, F. Gándara, et al., J. Am. Chem. Soc. 139 (2017) 13166–13172.
[24] Y. Liu, Y. Ma, J. Yang, et al., J. Am. Chem. Soc. 140 (2018) 16015–16019.
[25] D.L. Cockriel, J.M. McClain, K.C. Patel, et al., Inorg. Chem. Commun. 11 (2008) 1–4.
[26] N.R. Wadhwa, N.C. Hughes, J.A. Hachem, et al., RSC Adv. 6 (2016) 11430–11440.
[27] R. Dong, T. Zhang, X. Feng, Chem. Rev. 118 (2018) 6189–6235.
[28] I. Insua, J. Montenegro, J. Am. Chem. Soc. 142 (2020) 300–307.
[29] Y. Liu, J. Wan, X. Zhao, et al., Angew. Chem. Int. Ed. 62 (2023) e202302370.
[30] Z. Zhang, J. Zhao, Z. Guo, et al., Nat. Commun. 13 (2022) 1393.
[31] X. Zhang, K. Liu, J. Zhao, et al., J. Am. Chem. Soc. 144 (2022) 11434–11443.
[32] J. Zhao, M. Hong, Z. Ju, et al., Angew. Chem. Int. Ed. 61 (2022) e202214386.
[33] Y. Liu, X. Yan, Chem. Eur. J. 29 (2023) e202203365.
[34] G. Li, J. Zhao, Z. Zhang, et al., Angew. Chem. Int. Ed. 61 (2022) e202210078.
[35] S.L. Li, T. Xiao, C. Lin, et al., Chem. Soc. Rev. 41 (2012) 5950–5968.
[36] R. Van Hameren, A.M. Van Buul, M.A. Castriciano, et al., Nano Lett. 8 (2008) 253–259.
[37] U. Mansfeld, M.D. Hager, R. Hoogenboom, et al., Chem. Commun. 23 (2009) 3386–3388.
[38] A. Ajayaghosh, R. Varghese, V.K. Praveen, et al., Angew. Chem. Int. Ed. 45 (2006) 3261–3264.
[39] R. van Hameren, S.V. Lazarenko, J.W. Gerritsen, et al., Science 314 (2006) 1433–1436.
[40] M.M.L. Nieuwenhuizen, T.F.A. de Greef, R.L.J. van der Bruggen, et al., Chem. Eur. J. 16 (2010) 1601–1612.
[41] T. Mes, M.M.E. Koenigs, V.F. Scalfani, et al., ACS Macro Lett. 1 (2012) 105–109.
[42] H. Hofmeier, R. Hoogenboom, M. Wouters, et al., J. Am. Chem. Soc. 127 (2005) 2913–2921.
[43] L. Meazza, J.A. Foster, K. Fucke, et al., Nat. Chem. 5 (2013) 42–47.
[44] J. Zhang, S. Qi, C. Zhang, et al., Chem. Commun. 57 (2021) 6272–6275.
[45] C. Zhang, X. Deng, C. Wang, et al., Chem. Sci. 10 (2019) 8648–8653.
[46] J. Zhang, S. Qi, C. Zhang, et al., Org. Lett. 22 (2020) 7305–7309.
[47] J. Zhang, S. Qi, H. Yu, et al., Chin. Chem. Lett. 33 (2022) 4856–4859.
[48] T. Xiao, L. Zhou, X.Q. Sun, et al., Chin. Chem. Lett. 31 (2020) 1–9.
[49] T. Xiao, W. Zhong, W. Yang, et al., Chem. Commun. 56 (2020) 14385–14388.
[50] T. Xiao, L. Xu, J. Götz, et al., Mater. Chem. Front. 3 (2019) 2738–2745.
[51] T. Xiao, W. Zhong, L. Qi, et al., Polym. Chem. 10 (2019) 3342–3350.
[52] T. Xiao, L. Xu, J. Wang, et al., Org. Chem. Front. 6 (2019) 936–941.
[53] T. Xiao, J. Wang, Y. Shen, et al., Chin. Chem. Lett. 32 (2021) 1377–1380.
[54] J. Zhu, Z. Dong, S. Lei, et al., Angew. Chem. Int. Ed. 54 (2015) 3097–3101.
[55] C. Zeng, C. Zhang, J. Zhu, et al., Chin. J. Polym. Sci. 36 (2018) 261–265.
[56] R.P. Sijbesma, F.H. Beijer, L. Brunsveld, et al., Science 278 (1997) 1601–1604.